

Comparison of ground-based Brewer and FTIR total column O₃ monitoring techniques

M. Schneider¹, A. Redondas², F. Hase¹, C. Guirado², T. Blumenstock¹, and E. Cuevas²

¹IMK-ASF, Forschungszentrum und Universität Karlsruhe, Karlsruhe, Germany

²Centro de Investigación Atmosférico de Izaña, Agencia Estatal de Meteorología, Spain

Received: 24 September 2007 – Published in Atmos. Chem. Phys. Discuss.: 9 January 2007

Revised: 10 July 2008 – Accepted: 19 August 2008 – Published: 17 September 2008

Abstract. We compare the currently most precise, ground-based total O₃ measurement techniques: Brewer and FTIR. We give an overview of the similarities and the differences between the measurements and the retrieval approaches of both experiments. We compare coincident measurements performed at the Atmospheric Observatory of Izaña from 2005 to 2007 and demonstrate that, if the properties of the instruments are well characterised, the scatter between both experiments is as small as 0.5%. This is in agreement with the theoretical predictions and confirms empirically that both techniques are able to monitor total O₃ amounts with a precision of better than 0.4%. However, we found systematic differences between both techniques of around 4.5%, which we think are mainly due to discrepancies between the applied UV and infrared spectroscopic parameters.

1 Introduction

Over the last 20 years significant progress was made concerning the precision and accuracy of atmospheric remote sensing measurements. This development is due to improvements in both instrumental setups and in retrieval algorithms. High precision measurements performed on a continuous basis are needed in order to detect potential atmospheric trends as soon as possible. A good example is the atmospheric ozone content. In the coming decades some kind of ozone recovery is expected, however, it is difficult to predict how, when, and to what extent it will occur (Weatherhead and Andersen, 2006). Continuous high precision measurements of

O₃ are very important in this context. They provide for improved atmospheric O₃ models by detecting trends between the models and the measurements as soon as possible.

Currently there are two continuous ground-based measurement techniques that claim to monitor total O₃ with a precision of 1–2 DU: FTIR and Brewer. Their precision and accuracy are theoretically estimated in Schneider and Hase (2008) and Redondas and Cede (2006), respectively. Ground-based measurements are an important component of the global atmospheric monitoring system, since they are decisive for the validation of satellite data. Only space-based measurements achieve a continuous global coverage, but their quality is coupled to the precision and accuracy of the ground-based long-term reference experiments. In particular so-called “super-sites” play an important role in this context. They concentrate different measurement techniques at the same site offering a variety of parameters to be used for the validation of satellite data. In addition, these super-sites are very important for the development and quality assurance of the different ground-based experiments. The possibility to inter-compare the different ground-based techniques under routine conditions allows for the validation of new developments and for a timely identification of potential instrumental drifts. In this work we compare total O₃ amounts obtained from a state-of-the-art FTIR observing system and from the European reference Brewers. The measurements are performed at the Izaña Observatory, Canary Island of Tenerife, Spain. Currently the Izaña FTIR system provides the most precise FTIR O₃ data world-wide, which is due to both advanced instrumental equipment and an optimised O₃ retrieval strategy (Schneider and Hase, 2008). Concerning the Brewer, Izaña is the Regional Brewer Calibration Centre for Europe (<http://www.rbcc-e.org/>) of WMO/GAW (World Meteorological Organisation/Global Atmospheric Watch),



Correspondence to: M. Schneider
(matthias.schneider@imk.fzk.de)

which guarantees highest quality standards. Both FTIR and Brewer activities are part of NDACC (Network for Detection of Atmospheric Composition Change; Kurylo (1991, 2000); <http://www.ndacc.org/>). Currently, such high quality and continuously performed FTIR and Brewer measurements only coincide at the Izaña Observatory. Therefore, it is a predestinated site for an inter-comparison study of both techniques.

In the following we list the main similarities and differences of the FTIR and Brewer technique, and discuss their respective advantages and disadvantages (Sect. 2). In Sect. 1 we briefly introduce the site where the measurements used in this work were made. In Sects. 2 to 6 we compare operational data from two different Brewer spectrometers and the FTIR spectrometer. Finally, we summarise the reasons that make the Izaña data unique and conclude about the implications of our results (Sects. 7 and 8).

2 FTIR versus Brewer technique

The principle of both techniques is the same: both the FTIR and the Brewer spectrometer detect direct solar light. The experimental differences are the spectral regions that are analysed and the spectral resolution of the measurements. The respective retrieval algorithms deduce the atmospheric O₃ amounts by analysing the absorption signatures imprinted onto the extraterrestrial solar spectrum. For this purpose the Brewer and FTIR technique use different retrieval approaches, which are imposed by the nature of the respective experimental data.

2.1 The experiments

The Brewer spectrometer detects spectral irradiance in six channels in the UV (303.2, 306.3, 310.1, 313.5, 316.8, and 320.1 nm) each covering a bandwidth of 0.5 nm (resolution power $\lambda/\Delta\lambda$ of around 600). The spectral analysis is achieved by a holographic grating in combination with a slit-mask which selects the channel to be analysed by a photomultiplier. At Izaña only MK-III Brewer instruments with double monochromators are applied which widely reduces the impact of straylight on the measurements. The Brewer system works in a completely automatic way, and usually measures continuously during the whole day. The first channel at 303.2 nm is only used for spectral wavelength checks by means of internal Hg-lamps, the second channel is used for measuring SO₂ and the remaining four channels at longer wavelength determine the O₃ amounts. The finally reported O₃ result is the mean value of a set of 5 observations. The standard deviation within these 5 observations is used for the acceptance of the measurement, here we consider a measurement to be valid if this standard deviation is lower than 2.5 DU. The Brewer's field of view (FOV) is about 2.7° (diameter of solar disc is 0.5°). Consequently, all direct solar

irradiance is coupled into the spectrometer even for a moderate misalignment of the solar tracker. On the other hand, a certain fraction of the diffuse radiance (circumsolar) is measured together with the direct irradiance. This signal of the diffuse radiance increases with the amount of scattering, i.e. mainly with SZA and aerosols, and alters the retrieved O₃ amounts.

The Brewer experiment needs some instrumental characteristics to be determined by calibration experiments: the wavelength calibration and the slit function (instrumental line shape function), and the extraterrestrial constant (ETC). The slit function is determined once per year. This is done in a laboratory by means of low pressure discharge lamps (e.g. Fioletov et al., 2005; Gröbner et al., 1998). The exact wavelength settings are monitored in an automated mode every 40 min by means of the internal Hg-lamps. The slit function and the exact wavelength settings are necessary to convolve the highly resolved Bass and Paur (1985) O₃ absorption coefficients with the instrumental function. The ETC is the weighted sum of the logarithms of the intensity that would be detected by the different channels in the absence of any terrestrial atmosphere (according to Eq. 6 and text thereafter). The Izaña sky conditions allow the determination of the ETC for each Brewer independently by the Langley method. However, in this work we use the ETC transferred by the traveling world standard Brewer #017. This ETC calibration is done once per year. The traveling world standard is applied to guarantee a world-wide consistency within the Brewer network. The stability of the ETC calibration is monitored continuously in an automated mode using an internal halogen lamp. The difference between the weighted counts of the halogen lamp at the time of calibration and the smoothed mean of two weeks is used to correct the ETC (Fioletov et al., 2005).

The mid-infrared FTIR measurement program covers the spectral region from 700 to 4200 cm⁻¹ (corresponding to 14.3 to 2.4 μm), excluding the region between 1400 and 1700 cm⁻¹, which is not useful for ground-based measurements due to strong water vapour absorption. The spectral range is split up in 6 filter regions. For the longer wavelength region we use a band-pass filter for the 700–1400 cm⁻¹ region. The spectra are obtained by a Fourier analysis of the recorded interferograms. The spectral resolution depends on the maximum optical path difference between the interfering light beams. For operational O₃ measurements the FTIR spectra are measured with a resolution of 0.005 cm⁻¹, which corresponds to a resolution power $\lambda/\Delta\lambda$ at 1000 cm⁻¹ of 2×10^5 . The spectral windows applied for the O₃ retrieval are similar to those of (Schneider and Hase, 2008). They consist of a total of 3600 spectral bins and contain many individual O₃ rotational-vibrational lines (at 991.25–993.80 cm⁻¹, 1001.47–1003.04 cm⁻¹, and 1005.00–1006.91 cm⁻¹) and 4 CO₂ lines (at 962.80–963.80 cm⁻¹, 964.24–965.26 cm⁻¹, 967.20–968.21 cm⁻¹, and 968.59–969.60 cm⁻¹) of different intensity. The CO₂ signatures

allow the retrieval of a temperature profile which is expected to widely improve the precision of the retrieved total O₃ amount (Schneider and Hase, 2008). It is important to mention that all these individual rotational-vibrational lines are resolved: in the middle infrared the shape of absorption lines is dominated by pressure broadening with a typical HWHM of 0.04 cm⁻¹ at surface level, which is nearly one order of magnitude larger than the operational resolution of the FTIR spectrometer. The numerous fine-structured spectral features provide for an automatic wavelength calibration. The FTIR spectrometer has a field of view of only 0.2°, i.e. it only analyses sunlight coming from the center of the solar disc (diameter of 0.5°). Consequently, a misalignment of the solar tracker directly affects the observing geometry. In Schneider and Hase (2008) it is shown that for elevation angles below 20° this is the leading error source. Although on a much higher level of spectral resolution if compared to the Brewer, it is important to monitor the instrumental line shape (ILS) of the FTIR spectrometer. This is done regularly by performing low pressure cell calibration measurements as described in Hase et al. (1999). Even then the residual ILS error is estimated to be the most important error source concerning FTIR total O₃ amounts measured at solar elevation angles above 20°.

2.2 The retrieval approaches

The basic equation for analysing solar absorption spectra is Lambert Beer's law:

$$I(\lambda) = I_{\text{ET}}(\lambda) \exp(-\tau_{\text{O}_3}(\lambda) - \sum_x \tau_x(\lambda)) \quad (1)$$

Here $I(\lambda)$ is the measured intensity at wavelength λ , I_{ET} the extraterrestrial intensity, τ_{O_3} the optical depth due to O₃, and τ_x the optical depth due to all other atmospheric components (other trace gases, aerosols etc.). For O₃ it is:

$$\tau_{\text{O}_3}(\lambda) = \int \sigma_{\text{O}_3}(\lambda, s) n_{\text{O}_3}(s) ds \quad (2)$$

whereby $\sigma_{\text{O}_3}(\lambda, s)$ is the absorption cross section and $n_{\text{O}_3}(s)$ the concentration of O₃ at location s . The integration is performed along the path of the direct sunlight. The cross section σ_{O_3} depends on temperature and in the infrared additionally on pressure.

The integration of n_{O_3} perpendicularly throughout the atmosphere gives the total O₃ column amount (Ω_{O_3}):

$$\Omega_{\text{O}_3} = \int n_{\text{O}_3}(z) dz \quad (3)$$

To derive Ω_{O_3} from the measurements both techniques apply different approaches.

2.2.1 Principles of the Brewer retrieval

The Brewer algorithm considers the absorption by O₃ and SO₂, scattering by molecules, and extinction by aerosols. The algorithm applies an airmass factor (μ_x), according to:

$$\mu_x = \sec \left(\arcsin \left[\frac{R}{R+h_x} \sin \Theta \right] \right) \quad (4)$$

as the ratio between the slant and the vertical total column amount. Here R , Θ , and h_x are the Earth's radius, the apparent solar zenith angle (90° – elevation angle), and the effective altitude of the absorbing or scattering component ($h=22$ km for O₃, SO₂, and aerosols, and $h=5$ km for Rayleigh scattering). Equation (4) is a simplification of the real situation. It assumes that the absorbing compounds are concentrated at a single altitude h_x and it disregards that the refraction index depends on altitude. The errors produced by these assumptions are important for low solar elevation angles (for an elevation angle of 10° this error is 2–3% Bernhard et al., 2005).

Taking the logarithm of Eq. (1) and applying Eqs. (2) and (3) yields the following relation between the intensities at channel i (I_i) and the amount of the extinction components:

$$\log I_i = \log I_{\text{ET},i} - \sum_x \mu_x \sigma_x \Omega_x - \mu_{\text{O}_3} \sigma_{\text{O}_3} \Omega_{\text{O}_3} \quad (5)$$

The four channels at the longer wavelength are combined (Evans et al., 1987),

$$\sum_{i=1}^4 w_i \log I_i = \text{ETC} - \sum_{i=1}^4 w_i (\sum_x \mu_x \sigma_x \Omega_x + \mu_{\text{O}_3} \sigma_{\text{O}_3} \Omega_{\text{O}_3}) \quad (6)$$

and the weighting coefficients w_i are selected to minimise the influence of SO₂: $w_{[1;4]} = [1.0, -0.5, -2.2, 1.7]$. This choice also widely eliminates absorption features which depend in local approximation linearly on wavelength (λ) like Rayleigh scattering and aerosol extinction, since $\sum_{i=1}^4 w_i \lambda_i \approx \sum_{i=1}^4 w_i = 0$. In Eq. (6) we replaced $\sum_{i=1}^4 w_i \log I_{\text{ET},i}$, the extraterrestrial coefficient, by ETC. With the wavelength and slit function calibration we can calculate the convolved extinction coefficients (σ_x of Eq. 6). The ETC is transferred from a reference instrument (Fioletov et al., 2005). Changes with time in the sensitivity of the instrument are reflected in changes of this extraterrestrial coefficient. Equation (6) together with Eq.(4) provides the total vertical O₃ amount. For the derivation of Eq. (5) we have to assume a constant so-called effective σ_x throughout the atmosphere. Any temperature or pressure dependence is neglected. The “operational” algorithm applies a σ_{O_3} corresponding to an effective height of O₃ of 22 km and a fixed effective temperature of the O₃ layer of –45°C. These simplifications produce systematic and random errors. In the case of the Izaña Observatory the effective height is about the same as the one used by the operational algorithm, but the effective temperature ranges from –50°C in winter months to –45°C in summer months. With the parameterisation of Van Roozendaal et al. (1998) we expect a typical error of –0.4% during the summer months due to these simplifications.

Table 1. Main differences between Brewer and FTIR experiments.

	Brewer	FTIR
number of channels/spectral bins	4	3600
resolution power	6×10^2	2×10^5
measured wavelength regions	UV	mid-infrared
line-of-sight	“simplified” considerations	ray tracing model
field-of-view	2.7° (larger than solar disc)	0.2° (smaller than solar disc)
wavelength calibration	important: due to low resolution of measured spectra and very fine-structured σ_{O_3}	not necessary: high resolution spectra is self-calibrating
slit function (or ILS) calibration	important to calculate the convolved σ_x	important to correctly simulate convolved spectra
intensity calibration	not important: algorithm bases on ratio of channels	not necessary: highly resolved solar absorption measurements are self-calibrating with respect to spectral broadband structures
determination of ETC	is determined from a set of measurements (Langley plot or transferred from standard instrument)	not required
T dependence of σ_{O_3}	not considered (uses effective σ_{O_3})	fully considered as well as pressure dependency of σ_{O_3}
measurement frequency	very high, every 5 min during whole day (for solar elevation angle $> 10^\circ$)	only 1–2 measurements per day, on typically 3 days per week
O ₃ isotopologues	no separation of distinct isotopologues	measures $^{48}\text{O}_3$, asymmetric and symmetric $^{50}\text{O}_3$ and $^{49}\text{O}_3$ individually
size/mobility	small instrument, highly-mobile, best-suited as mobile reference instrument	large instrument, installed inside container, limited mobility
price	150 kEUR	500 kEUR

2.2.2 Principles of the FTIR retrieval

The FTIR retrieval (PROFFIT, Hase et al., 2004) applies a precise radiative transfer model (KOPRA, Höpfner et al., 1998; Kuntz et al., 1998; Stiller et al., 1998). KOPRA is a line-by-line model which simulates the measured spectra. It includes a ray tracing module (Hase and Höpfner, 1999) to simulate how the solar light passes through the atmosphere. The model uses a discretised atmosphere (here we apply 41 levels between the Earth surface and the top of the atmosphere). The optical depth for each layer, enclosed between a pair of adjacent levels, is calculated by performing the integration of Eq. (2) between two levels. The applied absorption cross section σ for each individual line and level are parameterised according to the HITRAN spectroscopic database (Rothman et al., 2005). The parameterisation takes care of the pressure and temperature dependency of σ , i.e. it depends on the pressure and temperature actually present at the corresponding level. Summing up the τ values of the different layers leads to the simulated spectra at the location of the observer (combination of Eqs. 1 and 2). The radiative transfer model determines the changes in the spectral fluxes y for a changing state vector x . These derivatives are sampled in a Jacobian matrix \mathbf{K} :

$$\partial y = \mathbf{K} \partial x \quad (7)$$

Inverting \mathbf{K} of Eq. (7) would allow an iterative calculation of the atmospheric state from the measurement alone. However, generally the problem is under-determined, i.e. the columns of \mathbf{K} are not linearly independent. To overcome this problem an optimal estimation (OE) approach is applied (Rodgers, 2000): since the actual atmospheric state cannot be determined unambiguously from the measurement the OE approach determines the most probable state for the given measurement. The approach is based on the Bayesian theorem and consists in maximizing a total probability density function (pdf). The total pdf is the product of two pdfs: a first, describing the probabilities of the residuals of the spectral fit, and a second, describing the a-priori known probabilities of the absorbers’ distributions.

This approach produces vertical O₃ concentration profiles ($n_{\text{O}_3}(z)$) for several O₃ isotopologues ($^{48}\text{O}_3$, asymmetric and symmetric $^{50}\text{O}_3$ and $^{49}\text{O}_3$) individually, since each isotopologue offers distinct absorption lines. The total column amounts are subsequently calculated by Eq. (3). In addition, the measured spectrum contains sufficient information to determine the main issues of the actual temperature profile. Actually the O₃ retrieval consists of a joint OE of O₃, $^{50}\text{O}_3$ / $^{48}\text{O}_3$, interfering species, and temperature profiles. Further details about the O₃ FTIR retrieval and its error budget are given in Schneider and Hase (2008). In the following

sections we always refer to the sum of all O₃ isotopologues when we talk about the FTIR O₃ amounts.

Applying highly-resolved infrared spectra it is easy to separate the extraterrestrial component from the fine-structured absorption signatures of atmospheric trace gases. In the infrared the solar radiation is reasonably close to a black body radiation at 6000 K, i.e. it has a rather smooth dependence on wavelength. The presence of the few solar lines causes no significant problem, since they are well known (e.g. Hase et al., 2006) and fully resolved by the FTIR spectrometer.

The spectral windows applied for the FTIR retrieval contain many spectral bins between the fine-structured absorptions of atmospheric trace gases to construct an empirical background continuum.

2.3 Summary

Table 1 collects the principle differences of both techniques and resumes their respective advantages. The Brewer technique depends on several calibration experiments: (a) the wavelength setting and slit function calibration. The convolved absorption cross sections strongly depend on this calibrations. (b) The transfer of the extraterrestrial constant (ETC) from the world standard Brewer. The ETC is necessary to separate the extraterrestrial from the atmospheric signal. Errors in the ETC add directly to the slant column amounts (see Eq. 6), i.e. they are especially important for low slant column amounts. On the other hand, every single FTIR spectrum is self-calibrating with respect to the wavelength and intensity: (a) the FTIR spectrometer fully resolves many rotational-vibrational lines, it provides for a very accurate and automatic wavelength calibration of the measured spectra. (b) the extraterrestrial spectrum can be easily simulated and there is sufficient information to derive the overall instrumental transmittance from every single measurement. Nevertheless, for high precision measurements of absorbers with sharp signatures (stratospheric absorbers), it is important to monitor the actual ILS of the FTIR instrument continuously. For elevation angles above 20° the remaining ILS uncertainties are the leading error source.

The Brewer algorithm applies the same σ_{O_3} throughout the year and throughout the whole atmosphere. It, furthermore, assumes a O₃ profile where all O₃ is concentrated in a single layer at 22 km. The FTIR retrieval, on the other hand, takes into account the actual O₃ and temperature profile and applies different σ_{O_3} s and temperatures for 41 different atmospheric levels. This is important, since σ_{O_3} depends on temperature and pressure. Furthermore, the FTIR retrieval uses a comprehensive ray tracing model.

The field-of-view of the Brewer instrument is rather large so perfect tracking is less important. However, it simultaneously analyses a significant amount of diffuse light, which is an important error source for low elevation angles. The field-of-view of the FTIR is smaller than the solar disc. For low

elevation angles (below 20°) the FTIR data quality depends critically on a perfectly working solar tracker.

A great advantage of the Brewer technique is that the measurements are performed with a very compact and mobile instrument and that all measurements including the calibrations are made nearly automatically. The measurements are performed continuously at many sites over the globe. For these reasons Brewer O₃ data are often used as reference in inter-comparison studies between different instruments and techniques, including space-based instruments. FTIR spectrometers only have limited mobility. They are generally installed inside a laboratory or a big shipping container. On the other hand, they are very versatile instruments measuring a great variety of atmospheric species. Concerning O₃, the FTIR measurements allow the different isotopologues to be distinguished. FTIR measurements at Izaña are typically performed three times per week.

3 The Izaña super-site

The Brewer and FTIR measurements are performed at the Izaña Observatory, which is located on the Canary Island of Tenerife, 300 km from the African west coast at 28°18' N, 16°29' W at 2370 m a.s.l. The Izaña Observatory is run by the Spanish Weather Service (Agencia Estatal de Meteorología). It is a World Meteorological Organization (WMO) Global Atmospheric Watch (GAW) station of global importance, and there are many different institutes from different countries involved in its manifold measurement program: in-situ measurements of O₃, CO₂, CO, CH₄, N₂O, NO_x, SO₂, SF₆, . . . , different in-situ analysers and filter radiometer to determine optical, physical and chemical properties of aerosols. In March 2001 Izaña's ECC-sonde, DOAS, Brewer and FTIR activities were accepted by the NDACC (Network for Detection of Atmospheric Composition Change, formerly called NDSC: Network for Detection of Stratospheric Change Kurylo (1991, 2000); <http://www.ndacc.org/>).

The Brewer measurements at Izaña started in May 1991. Since November 2003 they represent the Regional Brewer Calibration Centre for Europe (<http://www.rbcc-e.org/>) of WMO/GAW (World Meteorological Organisation/Global Atmospheric Watch). This Calibration Centre is essential for a coordinated European Brewer network that is needed for both present and future consistency of ground-based total ozone observations and for validation of satellite instruments. Furthermore, it plays an important role in the development and testing of new measurement techniques for the whole Brewer network. The Brewer data are often used as a reference for validating other ground- and satellite-based instruments.

The FTIR activities started in January 1999: up to 2005 a Bruker IFS 120M FTIR spectrometer was used. Since January 2005, a Bruker IFS 125HR spectrometer has been in operation. Currently the IFS 125HR is the best performing

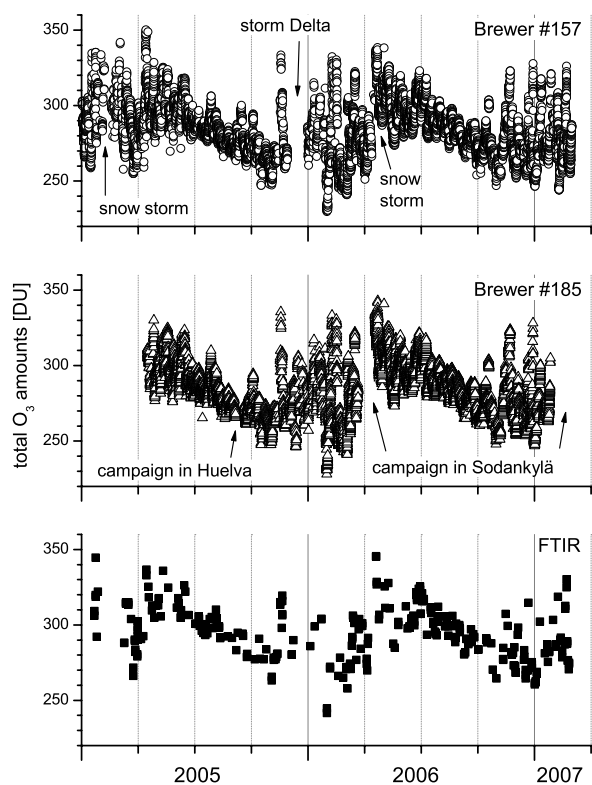


Fig. 1. Time series of total O₃ as measured by the site standard Brewer #157, the traveling standard Brewer #185, and the FTIR instrument.

high resolution FTIR spectrometer commercially available. Compared to the IFS 120M it has (a) a more stable instrumental line shape and (b) a 30% higher signal to noise ratio. In Schneider and Hase (2008) it is shown that a stable ILS is an important requisite to reach total O₃ precision of better than 1–2%. To guarantee highest quality of our FTIR O₃ products in this work, we only use O₃ amounts inverted from IFS 125HR measurements.

At the Izaña Observatory clean air and clear sky conditions are prevailing around all the year. Firstly, it is located in the region below the descending branch of the Hadley cell, typically above a stable inversion layer. Secondly, it is situated on an island far away from any significant industrial activities. Consequently it offers excellent conditions for atmospheric observations by remote sensing techniques and it is predestinated for calibration and validation activities. Due to its geographic location it is in particular valuable for the investigation of stratosphere-troposphere exchange associated with the subtropical jet (e.g. Kowol-Santen et al., 1999; Cuevas et al., 2007) and large scale transport from the tropics to higher latitudes.

Figure 1 shows the evolution of the total O₃ amounts in 2005 and 2006 as measured by the site standard Brewer #157,

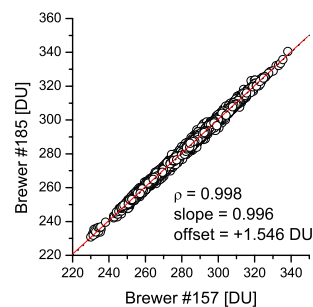


Fig. 2. Correlation between total column amounts of Brewer #157 and Brewer #185. Black circles are individual measurements, red line represents linear regression line of least squares fit.

traveling standard Brewer #185, and the FTIR instrument. The Brewer #185 started its operation in April 2005. Further gaps in the time series of the Brewer data are mainly due to intercomparison campaigns of the traveling standard Brewer #185: in September it was in Huelva, Spain; in March/April 2006 and January/February 2007 in Sodankylä, Finland. The gap in December 2005 is due to the (sub-)tropical storm Delta, which hit the island on 28 November. Peak gusts around 250 km/h were measured on this day and the Brewer #157 suffered some damage and was out of operation during the whole month of December 2005. Other gaps are due to power breakdown after snow storms in winter. The FTIR measures typically three times per week. The gap in February 2005 and the relatively sparse data in winter 2006 are due to snow storms or bad weather conditions.

4 Brewer #157 versus Brewer #185

In this section we compare total O₃ data from the site standard Brewer #157 and the traveling standard Brewer #185. Between January 2005 and February 2007 there are 4300 measurements performed simultaneously by both instruments. The correlation of these O₃ data is shown in Fig. 2. We find a correlation coefficient ρ of 0.998, a regression line slope of 0.996, and an offset of the regression line of 1.5 DU. The scattering around this regression line provides an estimate of the precision of the Brewer instrument with respect to O₃ amounts: The difference between both Brewer instruments is $0.2 \pm 0.4\%$. If we assume that the leading error sources of the O₃ amounts obtained from the two Brewer instruments are independent, we can estimate the precision of one Brewer instrument to $0.4/\sqrt{2} = 0.3\%$. However, it is likely that some error sources of two experiments which apply the same technique are correlated. Consequently the precision of 0.3% is only a best case estimation.

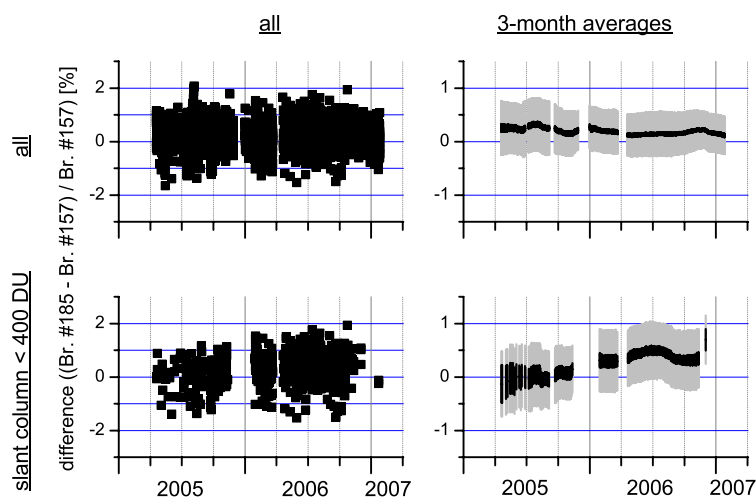


Fig. 3. Time series for the differences of total O₃ measured by the Brewer #157 and the Brewer #185 ($(\#185-\#157)/\#157$). Upper panels: for all coinciding measurements; bottom panels: for measurements with low slant columns (<400 DU). The left panels show all individual coincidences and the right panels the statistics of three month averages: the black shaded area covers the range within which the mean value is situated with a probability of 95%; the grey-shaded area indicates the standard deviation. The scale of the y-axis of the right panels is expanded by a factor 2.

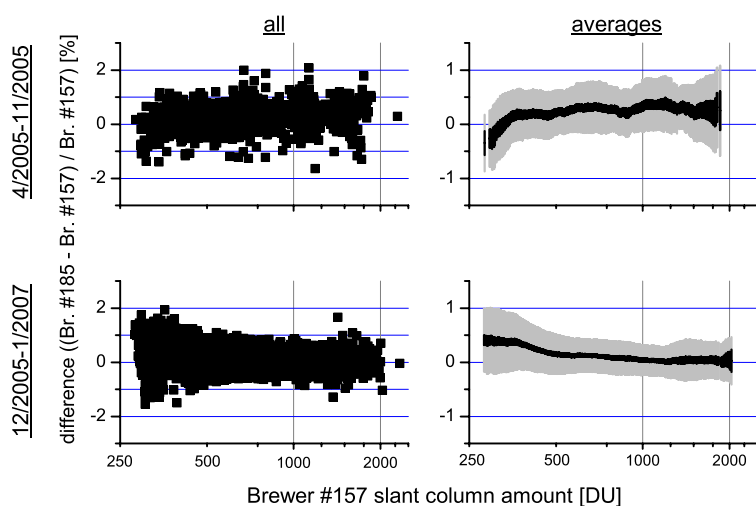


Fig. 4. Differences of total O₃ measured by the Brewer #157 and the Brewer #185 ($(\#185-\#157)/\#157$) versus slant column amount. Upper panel: for measurements between April and November 2005; bottom panel: for measurements between December 2005 and January 2007. The left panels show all individual coincidences and the right averages over values within a radius of 12.5% of the slant column amount: the black shaded area covers the range within which the mean value is situated with a probability of 95%; the grey-shaded area indicates the standard deviation. The scale of the y-axis of the right panels is expanded by a factor 2.

4.1 Temporal evolution

In the following we investigate how the difference between both Brewers evolves with time. The left panels of Fig. 3 depict the difference for all individual coincidences versus time. When contemplating this plot it is important to note

the scale on the y-axis. It is given in percent and consequently we are looking on temporal variations in the range of a few permil. Since the noise in the data is also situated in the permil range we can only expect to make some useful observations by contemplating averages over a certain amount of data. Here we average data over 3 months in the sense that

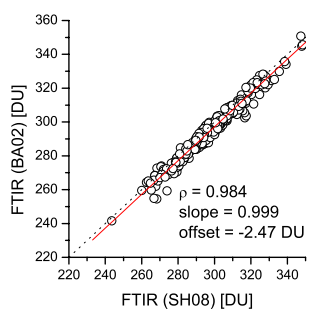


Fig. 5. Correlation between total column amounts for different FTIR approaches (a first similar to Barret et al. (2002) and a second according to Schneider and Hase, 2008). Black circles are the individual measurements, the red line is the linear regression lines of the least squares fit.

we apply data within a radius of 1.5 month around the considered date. The statistics of such averaged data are shown in the right panels. The grey bars represent the standard deviation (std) of the 3-month ensembles. They can be interpreted as overall precision of Brewer #157 and #185 within a three month period. The black bars represent the 95% confidence interval. This interval represents the area where the real mean value of a 3-month ensemble is situated with a probability of 95%. The radius of this area is approximately $2 \times \frac{\text{std}}{\sqrt{n}}$ (n is the number of ensemble members). Often $\frac{\text{std}}{\sqrt{n}}$ (the standard error of the mean) is used to determine the confidence radius. However, a so-calculated area would only contain the real mean with a probability of 68%. The upper panels show the situation if all 4300 coinciding Brewer measurements are applied. In this case even for the three month averages there is no significant temporal variation of the difference between the two Brewers. It seems that both instruments produce very consistent data even over several years. A small difference between 2005 and 2006 is that the overall precision of Brewer #157 and #185 for 3 month periods is slightly better in 2006 compared to 2005 (0.4% compared to 0.5%; see grey bars).

In addition we perform a separate analysis for low slant column amounts. This is done for two reasons: (1) FTIR measurements are generally performed at relatively low slant column amounts (75% of all FTIR measurements are at solar elevation angles above 35°). On the other hand, Brewer measurements are performed during the whole day, and thus, Brewer data include many O_3 amounts deduced from high slant column amounts. The separate analysis of low slant column assures that the Brewer data are characterised under similar condition as the FTIR data. (2) Systematic ETC errors are amplified for low slant column amounts, since a systematic error in the ETC produces a systematic bias in the retrieved slant column amounts (see Eq. 6). The bottom panels of Fig. 3 shows data only if the respective measurement was made for a slant column lower than 400 DU. This

slant column amount corresponds to an solar elevation angle of typically above 50° . Consequently, even at the subtropical site of Izaña, these data are not available in winter and the time series is limited to data from February to November. In these graphs we can observe a slight difference between 2005 and 2006. In 2005 both Brewers measure nearly the same, whereas in 2006 the site standard Brewer #157 produces O_3 amounts, which are around 0.5% lower than the Brewer #185 amounts. This observation is robust since it is based on more than 700 coincidences between the Brewers. The areas where the mean difference is situated with a probability of 95% (indicated by black bars in the left panels of Fig. 3) are separated for the years 2005 and 2006: we observe a slight systematic difference in the Brewers' performance between 2005 and 2006.

4.2 Dependence on slant column amounts

In the following we analyse in more detail the differences between the years 2005 and 2006. For this, we have a closer look at the dependence of the observed differences on the present slant column amounts. Figure 4 shows this dependence for the two periods: April 2005 to November 2005 and December 2005 to January 2007. The left panels show the individual data points. The right panels show statistics of the averages. Here the averages are calculated by including all data situated within a radius of 12.5% of the slant column amount, i.e. for a slant column amount of 500 DU we calculated the average of all data between 437.5 and 562.5 DU and for a slant column amount of 1000 DU we apply data between 875 and 1125 DU. The upper panels show the situation for the first period (1100 coincidences). There is a weak dependence of the difference between both Brewers on the slant column amount. For very low slant column amounts the Brewer #157 produces systematically larger amounts than the Brewer #185 (up to 0.5%) and for slant columns above 350 DU the sign changes and the #157 values are smaller than the #185 values. The lower panels show the situation for the year 2006 (period between December 2005 and January 2007; 3200 coincidences). It differs from the year 2005. Now for low slant column amounts the Brewer #157 data are 0.4% lower than the #185 amounts, and for slant columns above 600 DU both Brewer agree nearly perfectly. Furthermore, we found that in 2006 the data are less noisy than in 2005. These plots show that the inconsistencies between the Brewers with respect to 2005 and 2006 are reflected in a different dependence on the slant column amounts. Such a dependence indicates that there are weak inconsistencies in the ETCs applied for the Brewers (see Eq. 6). The dependence on the slant column amount is in particular large for 2005, indicating larger inconsistencies between both Brewers than in 2006.

5 FTIR (Barret et al., 2002) versus FTIR (Schneider and Hase, 2008)

In this Section we compare total O₃ data from two different FTIR retrieval approaches: first, using a method similar to Barret et al. (2002) (in the following called BA02) and second, similar to Schneider and Hase (2008) (in the following called SH08). By this means we perform an internal consistency check of the FTIR data. Figure 5 shows the correlation between the two approaches. Both retrievals apply the same O₃ absorption signatures but slightly different retrieval strategies. The first consists in an optimal estimation of O₃ profiles alone and the second in an joint optimal estimation of O₃, ⁵⁰O₃/⁴⁸O₃, and temperature profiles. A correlation coefficient of “only” 0.984 is relatively low. The agreement is poorer if compared to the agreement between both Brewer instruments. This is mainly due to errors from the BA02 method. In Schneider and Hase (2008) it was shown that the SH08 approach provides for significantly more precise data than the BA02 approach. It nearly eliminates the error due to uncertainties in the applied temperature profiles, which are the dominant error source of the BA02 approach. On the other hand, the SH08 approach is more sensitive to errors due to ILS uncertainties (Schneider and Hase, 2008). By comparing the data of both approaches we expect to get some information about the stability of the ILS from 2005 to 2007.

5.1 Temporal evolution

The temporal evolution of the difference between the two FTIR retrieval approaches is depicted in Fig. 6. Like for Fig. 3 the left panels show the individual measurements and the right panels show the statistics for the 3-month averages: the black bars represent the range of the mean values at a 95% confidence level, the grey bars represent the standard deviation. The upper panels show all data and the bottom panels only data for slant column amounts below 400 DU. First of all there is much more noise on the data when compared to Fig. 3. The relatively large noise is mainly due to temperature errors present in the BA02 approach. Again it should be remarked that the BA02 approach does not fully exploit the potential of the FTIR measurements. It is not an optimised approach, but we can exploit its different ILS sensitivity to perform an internal estimation of the FTIR's ILS characterisation. This internal estimation is achieved by averaging over a certain amount of data. This process significantly reduces the temperature error, which is mainly a random error. The remaining systematic signal should then be due to a systematic error source, for which both retrieval approaches have different sensitivities: e.g. the ILS error. The statistics of 3-month averages are depicted in the right panels of Fig. 6. We observe some systematic differences between the years 2005 and 2006/2007. First, the year 2005 is much more variable, which may indicate that the ILS of the

FTIR instrument is less stable than in 2006/2007. Second, the difference between both approaches is larger in 2005 than in 2006/2007 (1.5% compared to 0.8%). Assuming that the amplitude of the difference follows the amplitude of the remaining ILS error means that in 2005 the ILS is less well characterised than in 2006/2007. The bottom right panel of Fig. 6 shows the situation for slant column amounts below 400 DU. Here the differences are especially large in October 2005 (up to 2.2%). Furthermore, we observe that the difference increases from April to October 2005. We think that these observations indicate a gradual decrease of the ILS performance during 2005.

There are several possible explications for the relatively poor instrumental stability in 2005. In January 2005, after the installation of the instrument, the ILS was very well characterised (difference between BA02 and SH08 data of 0%). However, in the following there was a sequence of experimental complications. The setting of the ground or the whole surface below the container may have still been in progress during the first months of the measurements. In February 2005 there was a snow storm in Izaña and a subsequent breakdown of the power supply for several days. As a consequence the temperature in the container decreased to around 0°C. These mechanical and thermal stresses may have produced a degradation of the optical alignment. Furthermore, the low temperature damaged the hygroscopic entrance windows which had to be replaced. Unfortunately we only performed two independent ILS calibration measurements between January and November 2005. This is definitively not sufficient for a high quality characterisation of the ILS, in particular if we consider the aforementioned adverse conditions. In November 2005 we installed new firmware and reinstalled the detectors for technical servicing. The latter significantly reduced a channeling of 0.58 cm⁻¹. Since December 2005 the instrument is operating continuously and there were no further modifications necessary. In particular there was no further significant temperature breakdown inside the measurement container. Since the end of 2005 it is kept continuously at 22°C.

5.2 Dependence on slant column amounts

The ILS error of the FTIR O₃ data slightly depends on the O₃ slant column amount (Schneider and Hase, 2008). The error is larger for low slant column amounts than for high slant column amounts. Since the BA02 and SH08 approach have different ILS error sensitivities, this dependence should be observable in the difference of BA02 and SH08 O₃ amounts. Figure 7 depicts the dependence of the difference between BA02 and SH08 O₃ on the slant column amount. In 2005 (upper panels) we observe a clear increase of the negative difference for low slant column amounts, whereas in 2006 this increase is much smaller. Thus, Fig. 7 confirms our conclusions drawn from Fig. 6: in 2005 the FTIR instrument is less well characterised than in 2006.

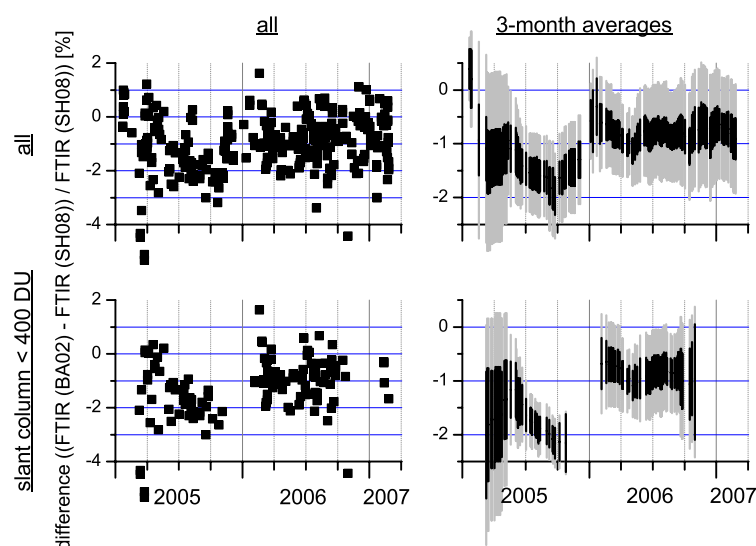


Fig. 6. Time series for the differences between the different FTIR approaches ($\text{FTIR (BA02)} - \text{FTIR (SH08)} / \text{FTIR (SH08)}$). Content of panels, symbols, and colours is the same as in Fig. 3.

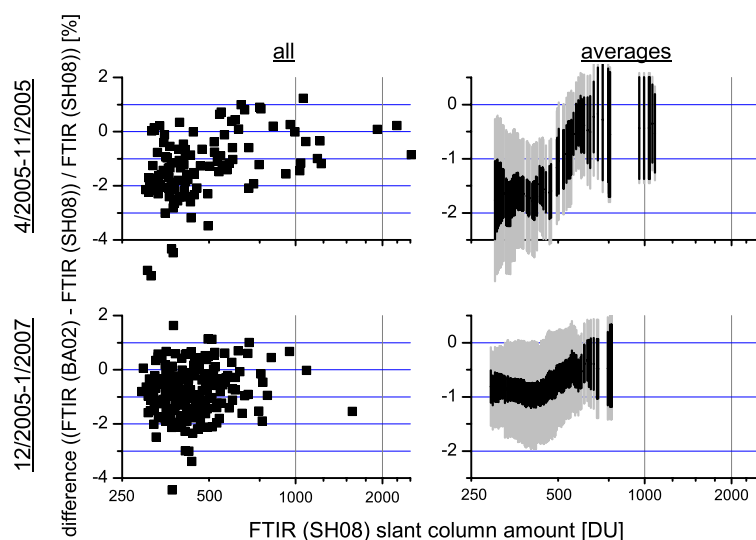


Fig. 7. Differences of total O_3 measured by the different FTIR approaches ($\text{FTIR (BA02)} - \text{FTIR (SH08)} / \text{FTIR (SH08)}$) versus slant column amounts. Content of panels, symbols, and colours is the same as in Fig. 4.

6 Brewer versus FTIR

In this section we compare total O_3 measurements of Brewer and FTIR. To exclude influences due to temporal variabilities we require that both Brewer and FTIR measurements should coincide within 30 min. Between January 2005 and February 2007 we identified a total of 305 FTIR measurements which fulfill these coincidence criteria with the Brewer measurements: 240 for the Brewer #157, 165 for the Brewer #185. Both Brewer instruments measure generally during the whole day. Figure 8 depicts the correlation between the site standard Brewer #157 and the FTIR O_3 amounts. Within all

240 coincidences we found one day which clearly is an outlier (2 March 2006; marked by blue circle in both panels of Fig. 8). So far we have no explanation for this outlier. We do not consider this data point for the following analysis since it is not representative but would widely influence the results. The left panel of Fig. 8 shows the correlation between the Brewer data and the FTIR data obtained from the BA02 approach. The agreement between the Brewer and these FTIR data is quite good: a correlation coefficient of 0.982 and a difference of $4.0 \pm 1.1\%$. This agreement is much better than reported by other studies (e.g. Barret et al., 2002; Schneider et al., 2005). It demonstrates the high quality of the Brewer

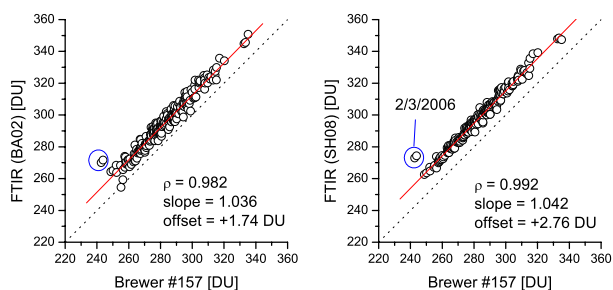


Fig. 8. Correlation between total column amounts of Brewer #157 and FTIR. Black circles are individual measurements, red lines linear regression lines of least squares fits. Left panel: correlation between Brewer and BA02 FTIR retrieval; right panel: correlation between Brewer and SH08 FTIR retrieval.

and FTIR measurements performed at Izaña. In particular, it confirms the potential of the FTIR technique when the instrumental aspects of the recipe as presented in Schneider and Hase (2008) are considered.

However, there is still a large potential to further improve the agreement. As shown in Schneider and Hase (2008) the BA02 error budget is dominated by errors in the assumed temperature profiles and applying the SH08 approach should widely reduce the overall FTIR errors. The correlation of the FTIR SH08 data with the Brewer #157 data is shown in the right panel of Fig. 8. It yields a correlation coefficient of 0.992. The difference between both instruments is $4.9 \pm 0.7\%$. The SH08 data agree significantly better with the Brewer data than the BA02 data. If we only correlate Brewer and FTIR SH08 data measured after November 2005 we get an even larger improvement. Then the correlation coefficient for the SH08 approach is 0.996 and the difference $-4.7 \pm 0.5\%$, whereas the BA02 approach only yields a correlation coefficient of 0.984 and a difference of $-4.0 \pm 1.0\%$ (Fig. 9). Limiting the comparison to measurements taken after November 2005 is justified since in 2005 the FTIR instrument is not optimally characterised (see Figs. 6 and 7 and discussion in Sect. 5).

The data measured after November 2005 reveal the real potential of the FTIR technique. Then the scatter between the FTIR (SH08) and the Brewer data is only 0.5%. This is an excellent value for two independent remote sensing experiments performed over more than 1 year. It can be interpreted as the root-square-sum of the precisions of the Brewer and FTIR instrument. As aforementioned the Brewer precision is not better than 0.3%. Consequently the Brewer/FTIR comparison is the empirical proof that the ground-based FTIR technique has the potential to measure O_3 amounts with a precision of better than 0.4%. For the BA02 approach the agreement does not improve significantly if we limit the comparison to data measured after November 2005. These data are dominated by errors caused by the assumed temperature

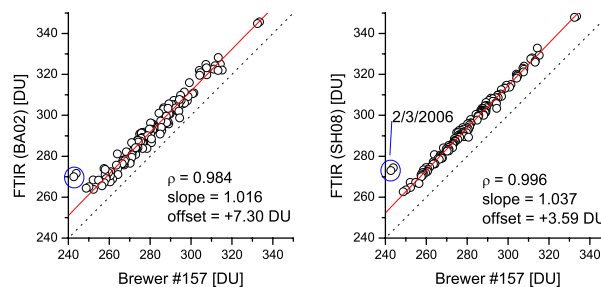


Fig. 9. Same as Fig. 8 but only applying data from December 2005 onward.

profiles, which are much larger than the errors caused by inconsistencies in the instrument's performance.

The Brewer-FTIR comparison confirms the theoretical prediction of Schneider and Hase (2008). However, there are significant systematic differences between both datasets: the FTIR observing system measures systematically 4.7% more O_3 than the Brewer system. These systematic differences may be due to incorrect characterisations of the instruments, simplifications in the Brewer retrieval algorithm, or discrepancies between the applied infrared (Rothman et al., 2005) and UV spectroscopic parameters (Bass and Paur, 1985).

Figure 10 shows the temporal evolution of differences between Brewer #157 and the FTIR data obtained by the SH08 approach. The upper panels show the data from all 240 coinciding measurements. Here the 95% confidence ranges (black bars in right panels) are much broader than in Fig. 3 due to a much smaller number of individual measurements applied for averaging. We observe clear differences between 2005 and 2006. In March 2005 FTIR O_3 amounts are typically 5.7% higher than Brewer #157 amounts, while in 2006 these differences are typically 4.6%. We observe a continuous increase of the Brewer #157 O_3 with respect to the FTIR O_3 between March and November 2005. The stability of the agreement since the end of 2005 until February 2007 is remarkable. Both techniques agree within 0.5% during more than 14 months. This excellent agreement is also achieved in 2005 if we consider only 3-month periods (see grey bars in right panels). Only in January and October/November 2005 it is larger. In both situations the ensembles include data for different FTIR and Brewer instrumental characteristics: the internal FTIR check (Fig. 6) shows steps in February and November 2005 and the internal Brewer check (Fig. 3) shows a step in December 2005. If we limit to slant column amounts below 400 DU (bottom panels) we make the same observations: within 3-month periods the data agree always within 0.5% and starting with January 2006 the agreement keeps stable over more than one year. Concerning the differences between 2005 and 2006 the continuous increase during 2005 is even more pronounced if compared to the upper panels (from -6.0% to -4.8%).

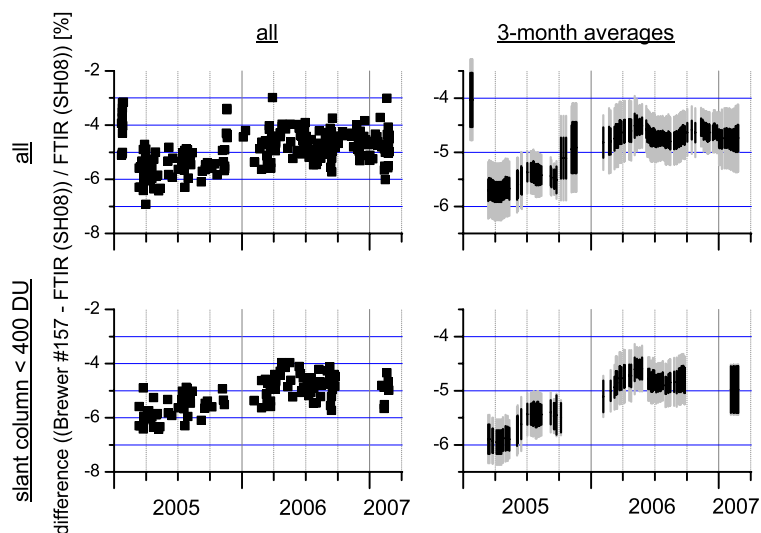


Fig. 10. Time series for the differences of total O₃ measured by the Brewer #157 and the FTIR. ((#157–FTIR)/FTIR). Content of panels, symbols, and colours is the same as in Fig. 3.

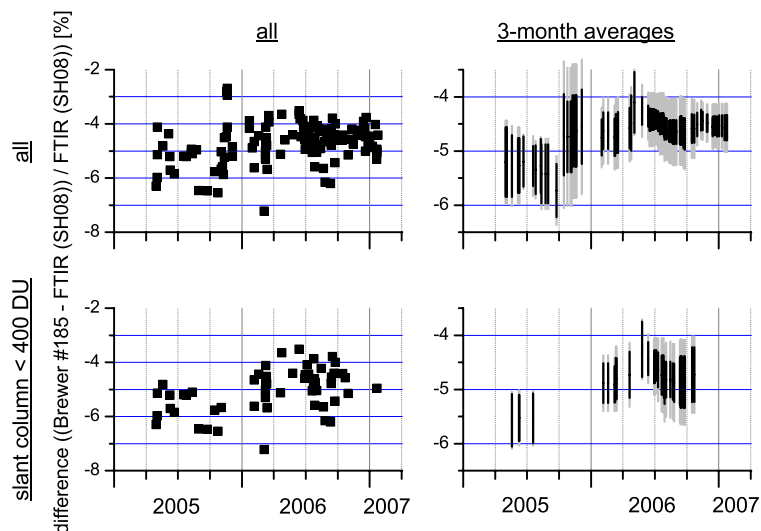


Fig. 11. Time series for the differences of total O₃ measured by the Brewer #185 and the FTIR. ((#185–FTIR)/FTIR). Content of panels, symbols, and colours is the same as in Fig. 3.

Finally, Fig. 11 depicts the temporal evolution of the difference between Brewer #185 and FTIR. As before, we observe a clear difference between 2005 and 2006. In 2005 the FTIR measures typically around 5.5% larger amounts than the Brewer #185. In 2006 the difference reduces to typically 4.8%. An interesting detail of Figs. 10 and 11 is the tendency to increased differences in the summer months (July and August). In summer 2005 there is a kind of intermission in the trend towards reduced Brewer-FTIR differences and in summer 2006 the difference is temporarily more negative than in April or October of the same year. This feature may be produced by the Brewer algorithm's assumption of a fixed effective O₃ temperature (see end of Sect. 2.2.1).

6.1 Temporal evolution

Figures 10 and 11 have many similarities but also two differences. Firstly, in 2005 the systematic overestimation of the Brewer O₃ amounts by the FTIR is slightly smaller for the Brewer #185 than for the Brewer #157. A reason could be that the differences in 2005 as observed in #185-FTIR are mainly due to inconsistencies in the FTIR data and the differences observed in #157-FTIR are due to both inconsistencies in the FTIR and the Brewer #157 data. Secondly, the #185-FTIR data are noisier than the #157-FTIR data. An elevated noise in the Brewer #185 data was already observed during the ETC calibration in October 2005

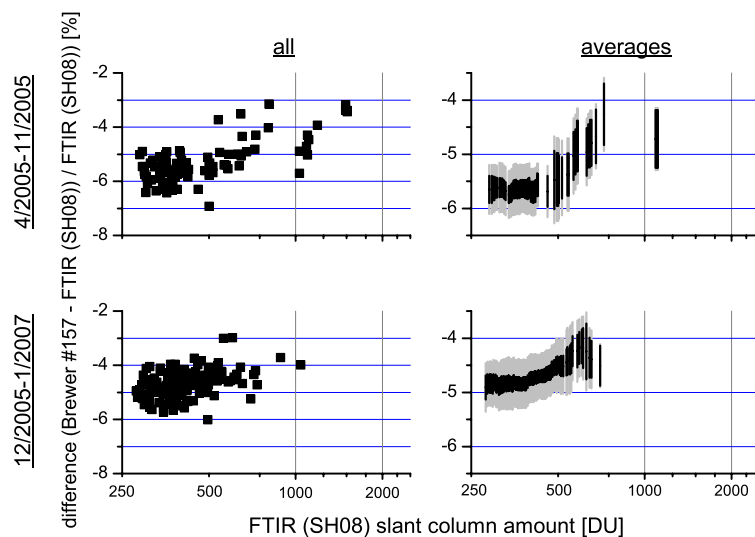


Fig. 12. Differences of total O_3 measured by the Brewer #157 and the FTIR. $((\#157-FTIR)/FTIR)$ versus slant column amounts. Content of panels, symbols, and colours is the same as in Fig. 4.

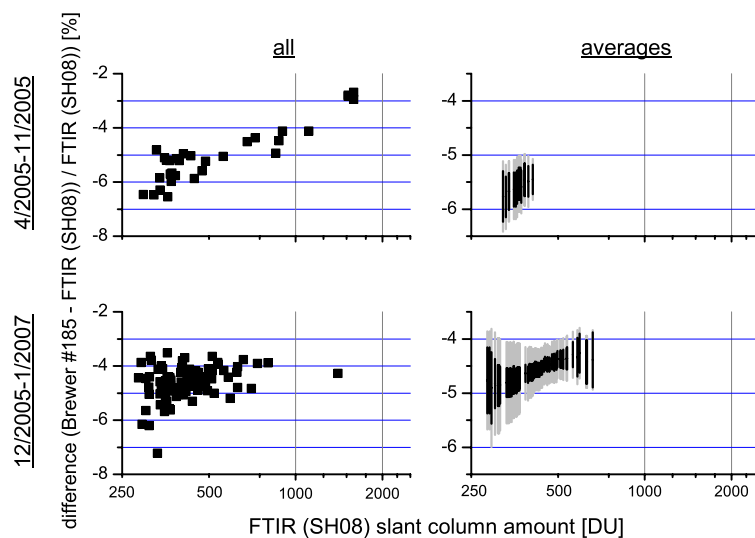


Fig. 13. Differences of total O_3 measured by the Brewer #185 and the FTIR. $((\#185-FTIR)/FTIR)$ versus slant column amounts. Content of panels, symbols, and colours is the same as in Fig. 4.

(K. Lamb, private communication) and is due to the internal filters applied by the Brewer instrument. There are five grey filters assuring that an adequate light intensity enters the photomultiplier (filter #1 is weakly attenuating and filter #5 is strongly attenuating). The problem is that these filters are not ideal grey filters, i.e. their attenuation depends weakly on wavelength. This not ideal attenuation is different for each filter and causes a filter dependent error in the retrieved O_3 amounts. The Brewer #185 is more sensitive than the Brewer #157. Even at large solar elevation angles the filter #3 is sufficiently attenuating for the Brewer #157, whereby the Brewer #185 frequently needs to switch between filter #3 and #4,

which is the reason for the elevated noise in the Brewer #185 data. It is possible to reduce this noise by correcting the error caused by the not ideal grey filters. This correction is not part of the standard retrieval algorithm, and thus not applied for the here presented data. The correction would also reduce the systematic difference of $(Brewer-FTIR)/FTIR$ by 0.5% (to around -4% in 2006/2007).

6.2 Dependence on slant column amounts

Figure 12 shows the dependence of the difference between the FTIR and Brewer #157 on the slant column amounts. The upper panels show the situation for all 106 coincidences

between January 2005 and November 2005. For increasing slant column amounts we observe a clear increase of the Brewer #157 O₃ amounts with respect to the FTIR amounts. At low slant columns the Brewer measures amounts which are 5.6% lower than the FTIR amounts. For slant column amounts at 700 DU this difference reduces to 4.4%. For the 2006 period the dependence on the slant column amount is less pronounced: at 700 DU the difference is around 4.5% and below 450 around 4.8%. This means that the FTIR and Brewer #157 data are more consistent in 2006 than in 2005. The upper right panel of Fig. 12 has significant similarities with the upper right panel of Fig. 7. This suggests that in 2005 the inconsistencies between the FTIR and Brewer #157 are mainly due to errors in the FTIR data.

Figure 13 shows the same as Fig. 12 but for the difference between FTIR and Brewer #185. We also found that dependence on slant column amounts is larger in 2005 if compared to 2006.

7 Some remarks on the quality of Izaña's O₃ measurements

Many other observatories could reach a similar precision as Izaña, but there is, to our knowledge, currently world-wide no other site where total O₃ column amounts are measured simultaneously by different ground-based techniques with the same high precision as presented in this work. The reasons for the currently unique high quality of the Izaña O₃ data are manifold: (a) the outstanding meteorological conditions that prevail at the Izaña Observatory benefit the quality of the FTIR measurements. There are only negligible intensity fluctuations while recording an FTIR interferogram. At less favorable measurement sites these fluctuations are larger due to changes of the atmospheric transparency (caused by clouds, short-scale inhomogeneities in water vapour, tropospheric aerosols, contrails etc.). These fluctuations are generally neglected, which produces errors in the retrieved O₃ amounts. To achieve an excellent FTIR data quality at less favorable sites the impact of the intensity fluctuations has to be reduced. Keppel-Aleks et al. (2007) describes a method to do so. (b) The application of state-of-the-art instrumentation. The Brewer triad is formed by three state-of-the-art instruments with double monochromator. Intercomparison studies with single monochromator instruments indicate a significantly poorer Brewer precision (Fioletov et al., 2005). The FTIR system consist of a very precise solar tracker (Huster, 1998), a Bruker IFS 125HR (stable ILS), and applies photo-voltaic detectors. These are the most important instrumental requirements needed for high precision FTIR measurements. Instabilities in the ILS are one of the dominant remaining error sources. These instabilities are responsible for the internal FTIR inconsistencies observed during 2005. (c) The high precision of both Brewer and FTIR depends on regularly performed calibration measurements. In case of the

Brewer, the ETC and wavelength are monitored internally by calibration lamps several times per day. Once per year the ETC is transferred from the traveling world standard Brewer. The slit function remains very stable. It is measured every year. In case of the FTIR, regularly performed ILS calibration measurements (Hase et al., 1999) are important. Since November 2005 these measurements are performed every 2–3 months. (d) Finally, it is important to apply an optimised retrieval algorithm: the FTIR only reaches a precision better than 0.5% if the retrieval strategy as proposed by Schneider and Hase (2008) is applied.

8 Summary and conclusions

The operational Brewer data presented here are very consistent over more than two years. Although, in 2005 the ETC determined for the Brewer #157 seems to be slightly less accurate than in 2006. However, these errors are very small and are in agreement with the expected ETC uncertainties. State-of-the-art Brewer instruments (double monochromator) combine high precision, stability, and mobility. They are perfectly suited for calibrating O₃ instruments at different sites. Furthermore, Brewer spectrometers are relatively economic and measure O₃ throughout the day and during the whole year.

The FTIR data presented here can be classified in two groups. A first group consisting of the data measured in 2005, when the instrument was not optimally characterised, and a second group consisting of the data measured after November 2005. The internal consistency check of Sect. 5 reveals the problems in 2005. The strong slant column dependence of the difference between the two FTIR retrieval approaches (Fig. 7) indicates the non optimal characterisation of the FTIR instrument. In 2005 the FTIR data do not represent the real potential of the FTIR technique. But even then we found a very small scatter with respect to the Brewer data of 0.8%. Since December 2005 the FTIR instrument is very well characterised. Then the scatter with respect to the Brewer data is only 0.5%, which confirms the prediction of Schneider and Hase (2008). This supports the theoretical quality assessments of other FTIR products, for which no direct empirical verification can be achieved. We think that our results are of particular interest in the context of ground-based high precision measurements of greenhouse gases, which are performed within TCCON (Washenfelder et al., 2006) and will serve for the validation of OCO (Crisp et al., 2004). TCCON aims for a precision of 0.1% in the O₂ corrected CO₂ column.

Our study empirically derives a precision of Izaña's Brewer and FTIR data of around 0.4%. The high precision provides unique opportunities for investigating systematic differences of both techniques and for studying atmospheric O₃ trends.

We find a significant systematic difference between the FTIR and Brewer data of 4–5%. Concerning the FTIR, a wrong ILS characterisation could produce a systematic error. This is the case in 2005, when an incorrect ILS produces an overestimation of the FTIR O₃ amounts of up to 1%. Concerning the Brewer, uncertainties in the ETC and slit function calibration or not ideal filters introduce systematic errors. An incorrect Brewer ETC assumptions as well as a wrong FTIR ILS characterisation would depend on the observed slant column amount. Such a dependence is clearly observed in 2005 but only very small in 2006 and 2007. Consequently, we conclude that the 2006/2007 data are less affected by systematic errors of instrumental nature. However, 0.5% of the difference of 4.5% as observed in 2006/2007 is caused by the non ideal internal Brewer filters (see end of Sect. 6.1). We think that in 2006/2007 in the worst case 1% of the observed systematic difference is due to errors in the assumed ILS, ETC, or non ideal filters. The rest is caused by the spectroscopic parameters. Our work indicates a systematic inconsistency between the infrared and UV spectroscopic coefficients of (4±1)%. This observation is in good agreement to the laboratory study of Picquet-Varrault et al. (2005).

For the study of the expected O₃ recovery, measurements which maintain a high precision over long time scales are needed. But even for regularly and carefully calibrated instruments small instrumental drifts may occur. In this context super-sites like Izaña are very important. The combination of different high quality experiments (like Brewer and FTIR) at a single site makes both experiments much more valuable for trend studies as if they were performed individually at different sites: the possibility to continuously inter-compare both techniques significantly reduces the risk of detecting artificial trends that may be caused by small instrumental drifts.

Acknowledgements. We would like to thank the European Commission and the Deutsche Forschungsgemeinschaft for funding via the projects GEOMON (contract GEOMON-036677) and RISOTO (Geschäftszeichen SCHN 1126/1-1), respectively. Furthermore, we are grateful to the Goddard Space Flight Center for providing the temperature and pressure profiles of the National Centers for Environmental Prediction via the automailer system. The Global Atmospheric Watch (GAW) Regional Brewer Calibration Center for Europe (RBBCC-E) is supported and maintained by the Spanish Agencia Estatal de Meteorología (AEMet). C. Guirado has enjoyed a grant from the AEMet (Resolución de 10-10-2006; BOE no. 279; 22-11-2006) at the Centro de Investigación Atmosférico de Izaña.

Edited by: A. Richter

References

- Barret, B., De Mazière, M., and Demoulin, P.: Retrieval and characterization of ozone profiles from solar infrared spectra at the Jungfraujoch, *J. Geophys. Res.*, 107, 4788–4803, 2002.
- Bass, A. M. and Paur, R. J.: The ultraviolet cross-sections of ozone, I. The measurements, in: *Atmospheric Ozone: Proceedings of the Quadrennial Ozone Symposium Held in Halkidiki, Greece, 3–7 September 1984*, edited by: Zerefos, C. S. and Ghazi, A., Springer, New York, 606–610, 1985.
- Bernhard, G., Evans, R. D., Labow, G. J., and Oltmans, S. J.: Bias in Dobson total ozone measurements at high latitudes due to approximations in calculations of ozone absorption coefficients and air mass, *J. Geophys. Res.*, 110, D10305, doi:10.1029/2004JD005559, 2005.
- Crisp, D., Atlas, R. M., Breon, F.-M., Brown, L. R., Burrows, J. P., Ciaia, P., Connor, B. J., Doney, S. C., Fung, I. Y., Jacob, D. J., Miller, C. E., O'Brien, D., Pawson, S., Randerson, J. T., Rayner, P., Salawitch, R. J., Sander, S. P., Sen, B., Stephens, G. L., Tans, P. P., Toon, G. C., Wennberg, P. O., Wofsy, S. C., Yung, Y. L., Kuang, Z., Chudasama, B., Sprague, G., Weiss, B., Pollock, R., Kenyon, D., and Schroll, S.: The orbiting carbon observatory (OCO) mission, *Adv. Space Res.*, 34, 700–709, 2004.
- Cuevas, E., Rodríguez, J. J., Gil, M., Guerra, J. C., Redondas, A., and Bustos, J. J.: Stratosphere-troposphere exchange processes driven by the subtropical jet, 7th EMS Annual Meeting/8th ECAM, EMS7/ECAM8 Abstracts, 4, EMS2007-A-00452, 2007.
- Evans, W. F. J., Fast, H., Forester, A. J., Henderson, G. S., Kerr, J. B., Vupputuri, R. K. R., and Wardle, D. I.: Stratospheric ozone science in Canada: An agenda for research and monitoring, Internal Rep. ARD-87-3, Atmospheric Environment Service, Toronto, Ontario, Canada, 128 pp., 1987.
- Fioletov, V. E., Kerr, J. B., McElroy, C. T., Wardle, D. I., Savastiouk, V., and Grajnar, T. S.: The Brewer reference triad, *Geophys. Res. Lett.*, 32, L20805, doi:10.1029/2005GL024244, 2005.
- Gröbner, J., Wardle, D. I., McElroy, C. T., and Kerr, J. B.: Investigation of the wavelength accuracy of Brewer spectrophotometers, *Appl. Optics*, 37, 8352–8360, 1998.
- Hase, F. and Höpfner, M.: Atmospheric raypath modelling for radiative transfer algorithms, *Appl. Optics*, 38, 3129–3133, 1999.
- Hase, F., Blumenstock, T., and Paton-Walsh, C.: Analysis of the instrumental line shape of high-resolution Fourier transform IR spectrometers with gas cell measurements and new retrieval software, *Appl. Optics*, 38, 3417–3422, 1999.
- Hase, F., Hannigan, J. W., Coffey, M. T., Goldman, A., Höpfner, M., Jones, N. B., Rinsland, C. P., and Wood, S. W.: Intercomparison of retrieval codes used for the analysis of high-resolution, ground-based FTIR measurements, *J. Quant. Spectrosc. Ra.*, 87, 25–52, 2004.
- Hase, F., Demoulin, P., Sauval, A. J., Toon, G. C., Bernath, P. F., Goldman, A., Hannigan, J. W., and Rinsland, C. P.: An empirical line-by-line model for the infrared solar transmittance spectrum from 700 to 5000 cm⁻¹, *J. Quant. Spectrosc. Ra.*, 102, 450–463, 2006.
- Höpfner, M., Stiller, G. P., Kuntz, M., Clarmann, T. v., Echle, G., Funke, B., Glatthor, N., Hase, F., Kemnitzner, H., and Zorn, S.: The Karlsruhe optimized and precise radiative transfer algorithm, Part II: Interface to retrieval applications, *SPIE Proceedings* 1998, 3501, 186–195, 1998.

- Huster, S. M.: Bau eines automatischen Sonnenverfolgers für bodengebundene IR-Absorptionmessungen, Diplomarbeit im Fach Physik, Institut für Meteorologie und Klimaforschung, Universität Karlsruhe und Forschungszentrum Karlsruhe, 1998.
- Keppel-Aleks, G., Toon, G. C., Wennberg, P. O., and Deutscher, N. M.: Reducing the impact of source brightness fluctuations on spectra obtained by FTS, *Appl. Optics*, 46, 4774–4779, 2007.
- Kowol-Santen, J., Ancellet, G., and Cuevas, E.: Analysis of Transport Across the Subtropical Tropopause, Proceedings for Fifth European Symposium on Stratospheric Ozone, St Jean de Luz (France), 27 September to 1 October 1999, p. 522, 1999.
- Kuntz, M., Höpfner, M., Stiller, G. P., Clarmann, T. V., Echle, G., Funke, B., Glatthor, N., Hase, F., Kemnitzer, H., and Zorn, S.: The Karlsruhe optimized and precise radiative transfer algorithm, Part III: ADDLIN and TRANSF algorithms for modeling spectral transmittance and radiance, *SPIE Proceedings 1998*, 3501, 247–256, 1998.
- Kurylo, M. J.: Network for the detection of stratospheric change (NDSC), *SPIE Proceedings 1991*, Remote Sensing of Atmospheric Chemistry, 1491 168–174, 1991.
- Kurylo, M. J. and Zander, R.: The NDSC – Its status after 10 years of operation, Proceedings of XIX Quadrennial Ozone Symposium, Hokkaido University, Sapporo, Japan, 167–168, 2000.
- Picquet-Varrault, B., Orphal, J., Doussin, J.-F., Carlier, P., and Flaud, J.-M.: Laboratory Intercomparison of the Ozone Absorption Coefficients in the Mid-infrared ($10\mu\text{m}$) and Ultraviolet (300–350 nm) Spectral Regions, *J. Phys. Chem. A*, 109, 1008–1014, 2005.
- Redondas, A. and Cede, A.: Brewer algorithm sensitivity analysis, SAUNA workshop, Puerto de la Cruz, Tenerife, November, 2006.
- Rodgers, C. D.: Inverse Methods for Atmospheric Sounding: Theory and Praxis, World Scientific Publishing Co., Singapore, ISBN 981-02-2740-X, 2000.
- Rothman, L. S., Jacquemart, D., Barbe, A., Benner, D. C., Birk, M., Brown, L. R., Carleer, M. R., Chackerian Jr., C., Chance, K. V., Coudert, L. H., Dana, V., Devi, J., Flaud, J.-M., Gamache, R. R., Goldman, A., Hartmann, J.-M., Jucks, K. W., Maki, A. G., Mandin, J.-Y., Massie, S. T., Orphal, J., Perrin, A., Rinsland, C. P., Smith, M. A. H., Tennyson, J., Tolchenov, R. N., Toth, R. A., Vander Auwera, J., Varanasi, P., and Wagner, G.: The HITRAN 2004 molecular spectroscopic database, *J. Quant. Spectrosc. Ra.*, 96, 139–204, 2005.
- Schneider M., Blumenstock, T., Hase, F., Höpfner, M., Cuevas, E., Redondas, A., and Sancho, J. M.: Ozone profiles and total column amounts derived at Izaña, Tenerife Island, from FTIR solar absorption spectra, and its validation by an intercomparison to ECC-sonde and Brewer spectrometer measurements, *J. Quant. Spectrosc. Ra.*, 91, 245–274, 2005.
- Schneider, M. and Hase, F.: Technical Note: Recipe for continuous monitoring of total ozone with a precision of 1 DU applying mid-infrared solar absorption spectra, *Atmos. Chem. Phys.*, 8, 63–71, 2008, <http://www.atmos-chem-phys.net/8/63/2008/>.
- Stiller, G. P., Höpfner, M., Kuntz, M., Clarmann, T. v., Echle, G., Fischer, H., Funke, B., Glatthor, N., Hase, F., Kemnitzer, H., and Zorn, S.: The Karlsruhe optimized and precise radiative transfer algorithm, Part I: Requirements, justification and model error estimation, *SPIE Proceedings 1998*, 3501, 257–268, 1998.
- Van Roozendaal, M., Peeters, P., Roscoe, H. K., De Backer, H., Jones, A. E., Bartlett, L., Vaughan, G., Goutail, F., Pommereau, J.-P., Kyro, E., Wahlstrom, C., Braathen, G., and Simon, P. C.: Validation of Ground-Based Visible Measurements of Total Ozone by Comparison with Dobson and Brewer Spectrophotometers, *J. Atmos. Chem.*, 29, 55–83, 1998.
- Weatherhead, E. C and Andersen, S. B.: The search for signs of recovery of the ozone layer, *Nature*, 441, 39–45, 2006.
- Washenfelder, R. A., Toon, G. C., Blavier, J.-F., Yang, Z., Allen, N. T., Wennberg, P. O., Vay, S. A., Matross, D. M., and Daube, B. C.: Carbon dioxide column abundances at the Wisconsin Tall Tower site, *J. Geophys. Res.*, 111, D22305, doi:10.1029/2006JD007154, 2006.